

\tilde{X}^1A_1 , \tilde{a}^3B_1 , \tilde{A}^1B_1 , and \tilde{B}^1A_1 Electronic States of PH_2^+ Timothy J. Van Huis,[†] Yukio Yamaguchi, C. David Sherrill,[‡] and Henry F. Schaefer III*

Center for Computational Quantum Chemistry, University of Georgia, Athens, Georgia 30602

Received: March 18, 1997; In Final Form: May 28, 1997[⊗]

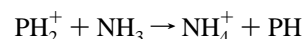
Four electronically low-lying states of PH_2^+ have been investigated using several different ab initio methods and multiple basis sets. This systematic study of both method and basis set provides reliable benchmarking for estimation when high levels of theory are not attainable. Self-consistent field (SCF), two-configuration self-consistent field (TCSCF), complete active space self-consistent field (CASSCF), configuration interaction with single and double excitations (CISD), and CASSCF second-order configuration interaction (SOC) levels of theory were employed with eight different basis sets of triple- ζ quality. Being the second root of the TCSCF, CASSCF, TCSCF–CISD, and CASSCF–SOC wave functions, the third excited state (\tilde{B}^1A_1) is of particular theoretical interest, for theoretical treatments of states not the lowest of their symmetry are traditionally very difficult. It is confirmed in this study that the four low-lying states of PH_2^+ all have bent structures and are of C_{2v} symmetry. Also determined in this study for these four electronic states were relative energies and physical properties including dipole moments and harmonic vibrational frequencies with their associated infrared (IR) intensities. These properties were compared with experimental values when possible. At the CISD level with the largest basis set (triple- ζ plus triple polarizations with two higher angular momentum and two diffuse functions [TZ3P(2f,2d)+2diff]), the equilibrium geometries of the four states are predicted to be $r_e = 1.415$ Å and $\theta_e = 93.1^\circ$ (\tilde{X}^1A_1), $r_e = 1.403$ Å and $\theta_e = 121.7^\circ$ (\tilde{a}^3B_1), $r_e = 1.417$ Å and $\theta_e = 124.7^\circ$ (\tilde{A}^1B_1), and $r_e = 1.411$ Å and $\theta_e = 159.3^\circ$ (\tilde{B}^1A_1). At this level of theory, the dipole moments of the ground and first three excited states of PH_2^+ are predicted to be 1.056 D (\tilde{X}^1A_1), 0.653 D (\tilde{a}^3B_1), 0.751 D (\tilde{A}^1B_1), and 0.324 D (\tilde{B}^1A_1), which are large enough to make these states susceptible to microwave spectroscopic analysis. The energy separations (T_0 values) between the ground (\tilde{X}^1A_1) and three excited states predicted at the CASSCF–SOC level with the TZ3P(2f,2d)+2diff basis set are 17.74 kcal/mol (0.77 eV, 6200 cm^{-1} : $\tilde{a}^3B_1 \leftarrow \tilde{X}^1A_1$), 45.82 kcal/mol (1.99 eV, 16 030 cm^{-1} : $\tilde{A}^1B_1 \leftarrow \tilde{X}^1A_1$), and 85.05 kcal/mol (3.69 eV, 29 750 cm^{-1} : $\tilde{B}^1A_1 \leftarrow \tilde{X}^1A_1$). After comparison of theoretical and experimental data for isovalent systems studied at the same level of theory, error bars for the $\tilde{B}^1A_1 \leftarrow \tilde{X}^1A_1$ splitting are estimated to be ± 1.5 kcal/mol (± 525 cm^{-1}). Adiabatic and vertical ionization potentials of PH_2 are also presented.

I. Introduction

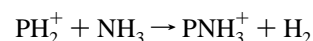
The PH_2^+ molecule is isovalent with CH_2 and NH_2^+ , and it shares several of these molecules' characteristics, one of which being a multitude of low-lying electronic states. Because of the controversies between theory and experiment surrounding methylene in the past,^{1–3} it has become *the* benchmark molecule around which many high-level ab initio methods were developed.⁴ Theoretical predictions for methylene are now considered nearly as reliable as experimental results,^{5–12} and relative energetic splittings between electronic states (e.g. $\tilde{a}^3B_1 \leftarrow \tilde{X}^1A_1$) now approach 0.1 kcal/mol accuracy.^{7,11–15} Because of this, it was assumed that theory applied to the many species isovalent with CH_2 (NH_2^+ , PH_2^+ , SiH_2 , GeH_2 , etc.)^{16–21} would yield predictions for these molecules which would be of similar quality. In particular, those molecules containing heavier atoms, such as P, Si, and Ge, can benefit greatly from such predictions, as experimental data on these species is difficult to obtain. This is especially true of the subject of this study, PH_2^+ ; the experimental data on the structure and properties of the ground or excited states of the gas-phase PH_2^+ molecule is very limited. This is due primarily to the difficulty of obtaining gas-phase ions in significant concentrations (because of their short lifetimes) in order to extract meaningful data.²² Therefore, the molecular parameters and energetic predictions that can be

gained from reliable theory are warranted to better equip spectroscopists in their efforts to characterize the PH_2^+ ion.

The PH_2^+ molecule has gained attention due to its connection to interstellar chemistry. The rise in interest in interstellar chemistry in recent years can be traced to an increased number of compounds detected in the interstellar medium, as well as the increased capabilities of experimentalists to characterize the reactions of these compounds. Theoretical studies have also boosted the understanding of interstellar compounds, due to the fact that ab initio predictions are best suited to molecules in the gas phase at absolute zero temperature. The detection of PN in interstellar clouds^{23,24} as well as the detection of phosphine (PH_3) in Jupiter's atmosphere²⁵ has greatly increased the interest in the ion–molecule chemistry of phosphorus compounds, particularly the hydrides. Such discoveries have led to kinetic studies of the ion–molecule reactions of the PH_n ($n = 1–4$) series, which have consequently shown that PH_2^+ is a likely candidate as an intermediate in these interstellar reactions.^{26,27} For example,



or

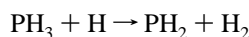


in which the second reaction is preferred over the first. The potential energy surface of the $PH_2^+ + CO$ reaction has been

[†] Abraham Baldwin graduate fellow.[‡] Current address: Department of Chemistry, Box 308, University of California, Berkeley, CA 94270-1460.[⊗] Abstract published in *Advance ACS Abstracts*, August 15, 1997.

the subject of a theoretical study by Esseffar, Luna, M6, and Y6ñez²⁸ with the hope to gain some insight into the thermodynamics of these interstellar-type reactions.

While experimental determinations of the properties of the PH₂⁺ ion have been rather limited, some notable work on the energy separations between low-lying states has been done. Edwards, Jackson, MacLean, and Sarre performed a laser photodissociation study of PH₂⁺ in which the yield of P⁺ ions was monitored as a function of the tunable dye laser frequency.³¹ They found a characteristic separation between bands of approximately 1200 cm⁻¹ which they attributed to the bending frequency of the ground state. In the same study, Edwards et al. also attempted to determine the $\tilde{A}^1B_1 \leftarrow \tilde{X}^1A_1$ energy separation, but were apparently unsuccessful due to noise from rotation bands.³¹ In 1986, Berkowitz, Curtiss, Gibson, Greene, Hillhouse, and Pople³² obtained an ion yield curve of PH₂⁺ from both the photoionization of PH₃ and the pyrolysis of benzylphosphine (C₆H₅CH₂PH₂). Although the spectrum contained a rather large signal-to-noise ratio, the authors were able to assign the first ion yield increase (i.e. the ionization potential of PH₂) at 1262.0 ± 1.0 Å (226.5 ± 0.05 kcal/mol, 79 220 ± 17 cm⁻¹) to the \tilde{X}^1A_1 state of PH₂⁺. The next increase in ion yield was assigned at approximately 1177 Å (242.9 kcal/mol, 84 960 cm⁻¹), and was defined as the lower limit to the energy levels of the \tilde{a}^3B_1 state, putting the singlet–triplet gap at ≥ 16.4 kcal/mol (5740 cm⁻¹). In 1989, Berkowitz and Cho³³ reinvestigated the photoion yield curve of PH₂⁺, obtaining an independent curve as the result of the photoionization of PH₂ from the following reaction:



Using a mass spectrometer, they were able to increase the signal-to-noise ratio and obtain more reliable results, which placed the singlet–triplet splitting at (*T*₀) 16.1 kcal/mol (5630 cm⁻¹). However, they did qualify their results, stating that the energy separation could be shifted by one vibrational quantum (2.3 kcal/mol, 0.1 eV, 800 cm⁻¹) without seriously affecting the interpretations. Therefore, the most reliable experimental singlet–triplet splitting to date is 16.1–18.4 kcal/mol.³³ Berkowitz and Cho³³ also tentatively assigned the next separation ($\tilde{A}^1B_1 \leftarrow \tilde{X}^1A_1$) at 44.3 kcal/mol (15 490 cm⁻¹). However, inspection of their published spectrum reveals that this is an estimation, as there is quite a large amount of noise surrounding this feature. To date, there has been no experimental determination of the geometric parameters of the ground and first three excited states of the PH₂⁺ molecule.

The theoretical work on PH₂⁺ is fairly extensive; however, most work has concentrated on the ground and first excited state.^{20,34–36} Cramer, Dulles, Storer, and Worthington²⁰ carried out a systematic study of singlet–triplet gaps, including that of PH₂⁺, at the complete active space self-consistent field (CASSCF), multireference configuration interaction (MRCI), and density functional theory (DFT) levels of theory using Dunning's³⁷ aug-cc-pVTZ (minus the f functions) basis set. Bruna and Peyerimhoff³⁸ determined the bending potential energy curves (at a constant P–H bond length of 1.40 Å) of the ground and several excited states at the DZP MRD-CI level; however, the state splittings yielded from their published curves do not appear to match the energy separations which they published³⁹ in another study. This may be due to the effect of optimizing the P–H bond for each state, but it is not clear if this is the case. Perhaps the most far-reaching study thus far has been that of Balasubramanian.¹⁸ Using a large triple- ζ basis which included both diffuse functions and higher angular momentum f- and g-type functions (13s10p3d2f1g/7s6p3d2f1g)

in conjunction with the CASSCF second-order configuration interaction (SOC) method, Balasubramanian was able to perform geometry optimizations of the ground (\tilde{X}^1A_1) and first two excited states (\tilde{a}^3B_1 and \tilde{A}^1B_1). From his results, he predicted (*T*_e values) 17.73 kcal/mol (6200 cm⁻¹) for the $\tilde{a}^3B_1 \leftarrow \tilde{X}^1A_1$ energy separation and 45.06 kcal/mol (15 760 cm⁻¹) for the $\tilde{A}^1B_1 \leftarrow \tilde{X}^1A_1$ separation. Recently, Bauer, Hirst, Batey, Sarre, and Rosmus carried out a CASSCF–MRCI study on PH₂⁺ using Dunning's correlation consistent basis sets (cc-pVQZ on P and cc-pVTZ on H).⁴⁰ They determined the theoretical potential-energy functions and spectroscopic data for the ground (\tilde{X}^1A_1) and second (\tilde{A}^1B_1) electronic states. On the basis of their data, they were able to obtain reliable potential energy surfaces and harmonic vibrational frequencies for these two states. To date, these have been the most reliable frequencies theoretically determined for this molecule.

The objective of this study is to examine systematically the ground and three excited states of PH₂⁺ using self-consistent field (SCF), two-configuration self-consistent field (TCSCF), CASSCF, SCF(TCSCF)–CISD, and CASSCF–SOC wave functions with eight different basis sets. This study is analogous to a work previously done in this group on CH₂,¹² in which the theoretically predicted energy separations between the ground and first three excited states (as well as the geometrical parameters) were found to be in excellent agreement with experiment. Also, the progression in levels of theory as well as in basis set size shown in our study provides a means for the estimation of molecular properties and energetics when these large levels of theory cannot be employed. While PH₂⁺ lacks as extensive an experimental and theoretical background as CH₂, important analogies can be drawn between the two which should allow for a greater understanding of these important (six valence e⁻) AH₂ systems. Also, the results of this study should assist further experimental characterization of the low-lying electronic states of PH₂⁺.

II. Electronic Structure Considerations

It is generally agreed^{18,20,31,33–36,38–40} that the \tilde{X}^1A_1 electronic state of the PH₂⁺ molecule is bent with *C*_{2v} symmetry, and, similar to the \tilde{a}^1A_1 state of both CH₂ and NH₂⁺, it may be qualitatively expressed as

$$[\text{core}](4a_1)^2(2b_2)^2(5a_1)^2 \tilde{X}^1A_1 \quad (1)$$

where [core] stands for

$$[\text{core}] = (1a_1)^2(2a_1)^2(1b_2)^2(3a_1)^2(1b_1)^2 \quad (2)$$

However, due to the low lying \tilde{B}^1A_1 state, it is perhaps better to represent the \tilde{X}^1A_1 state with a two-configuration wave function.

$$C_1[\text{core}](4a_1)^2(2b_2)^2(5a_1)^2 + C_2[\text{core}](4a_1)^2(2b_2)^2(2b_1)^2 \tilde{X}^1A_1 \quad (3)$$

The first and second excited states, \tilde{a}^3B_1 and \tilde{A}^1B_1 (although of different spin symmetry), can both be qualitatively presented by the electron configuration

$$[\text{core}](4a_1)^2(2b_2)^2(5a_1)(2b_1) \tilde{a}^3B_1, \tilde{A}^1B_1 \quad (4)$$

A minimal description of the \tilde{B}^1A_1 state requires at least a two-configuration wave function. Unlike its linear first-row analogue, $\tilde{c}^1\Sigma_g^+ \text{NH}_2^+$,⁴¹ the \tilde{B}^1A_1 state of PH₂⁺ is bent; thus (in *C*_{2v} symmetry)

$$C_1[\text{core}](4a_1)^2(2b_2)^2(2b_1)^2 + C_2[\text{core}](4a_1)^2(2b_2)^2(5a_1)^2 \tilde{B}^1A_1 \quad (5)$$

is a qualitative representation.

At this time it should be noted that for the \tilde{X}^1A_1 state, the CI coefficients, C_1 and C_2 , are of opposite signs, while the coefficients for the \tilde{B}^1A_1 state have the same sign. Also note for the \tilde{X}^1A_1 and \tilde{B}^1A_1 states $|C_1| > |C_2|$. The \tilde{B}^1A_1 state may be viewed as a doubly excited state with respect to the \tilde{X}^1A_1 state.

III. Theoretical Methods

Eight basis sets were used in this study, all of triple- ζ (TZ) quality. The TZ basis for P was derived from McLean and Chandler's TZ contraction⁴² of Huzinaga's primitive Gaussian functions⁴³ and is designated (12s9p/6s5p). The TZ basis for H was obtained from Dunning's TZ contraction⁴⁴ of Huzinaga's primitive Gaussian functions⁴⁵ and it is designated (5s/3s). The orbital exponents of the polarization functions were $\alpha_d(P) = 1.20$ and 0.300 and $\alpha_p(H) = 1.50$ and 0.375 for double polarization (TZ2P); and $\alpha_d(P) = 2.40$, 0.600 , and 0.150 and $\alpha_p(H) = 3.00$, 0.750 , and 0.1875 for triplet polarization (TZ3P). Six Cartesian d-like and 10 Cartesian f-like functions were used throughout.

The orbital exponents of the higher angular momentum functions were $\alpha_f(P) = 0.450$ and $\alpha_d(H) = 1.00$ for single higher angular momentum functions [TZ2P(f,d)] and $\alpha_f(P) = 0.900$ and 0.225 and $\alpha_d(H) = 2.00$ and 0.500 for double higher angular momentum functions [TZ3P(2f2d)]. The diffuse function orbital exponents were determined in an "even tempered sense" as a mathematical extension of the primitive set, according to the formula of Lee and Schaefer,⁴⁶ with $\alpha_s(P) = 0.034\ 63$, $\alpha_p(P) = 0.031\ 38$, and $\alpha_s(H) = 0.030\ 16$ for single diffuse functions (TZ2P+diff) and $\alpha_s(P) = 0.034\ 63$, $0.011\ 11$, $\alpha_p(P) = 0.031\ 38$, $0.011\ 61$, and $\alpha_s(H) = 0.030\ 16$, $0.009\ 247$ for double diffuse functions (TZ3P+2diff). The largest basis set, TZ3P(2f,-2d)+2diff, contained 119 contracted Gaussian functions with a contraction scheme of (14s11p3d2f/8s7p3d2f) for P and (7s3p2d/5s3p2d) for H.

The geometries of the lowest three electronic states were optimized via standard analytic derivative methods⁴⁷⁻⁴⁹ while it was necessary to optimize the geometry of the \tilde{B}^1A_1 state via finite differences of energy points. Harmonic vibrational frequencies and associated IR intensities were determined analytically for the lowest three states at the SCF⁵⁰⁻⁵³ and TCSCF^{54,55} levels of theory and by finite differences of analytic gradients for the CISD⁵⁶⁻⁵⁹ wave functions. It was necessary to obtain the harmonic vibrational frequencies and associated IR intensities for the \tilde{B}^1A_1 state by finite differences of energy points and dipole moments, respectively, at the TCSCF-CISD level of theory. It should be noted that geometrical parameters (bond lengths and bond angles) obtained by the energy point optimizations in this study are comparable to analytically optimized parameters to at least 10^{-7} , and vibrational frequencies are converged to the tenth of a cm^{-1} .⁶⁰ All computations were performed using the PSI 2.0 suite of ab initio quantum mechanical programs.⁶¹ Cartesian gradients were optimized to at least 10^{-6} au. The energies of SCF, CISD, and CASSCF wave functions were converged to 10^{-12} hartrees.

One-configuration SCF wave functions may be used to obtain the zeroth-order descriptions of the lowest three states. However, the \tilde{X}^1A_1 and \tilde{B}^1A_1 states may be more appropriately described as the first (eq 3) and second (eq 5) eigenvectors, respectively, of the TCSCF secular equation. Dynamical correlation effects were included by using SCF(TCSCF)-CISD,

CASSCF,⁶²⁻⁶⁴ and CASSCF-SOCI levels of theory. In all the CISD and SOCI procedures, the core (P 1s, 2s, and 2p-like) orbitals were frozen and a single virtual (P 1s*-like) orbital was deleted. With the TZ3P(2f,2d)+2diff basis set, the numbers of configuration state functions (CSFs) for the CISD wave functions in C_{2v} symmetry are 28 150 (\tilde{X}^1A_1 , TCSCF reference), 20 732 (\tilde{a}^3B_1 , SCF reference), 20 656 (\tilde{A}^1B_1 , SCF reference), and 28 150 (\tilde{B}^1A_1 , TCSCF reference). The CASSCF and CASSCF-SOCI energies were determined at the CISD optimized geometries with the same basis set. Two active spaces were selected for the CASSCF wave functions. The first, which we will denote as CAS I, comprised the six (valence) electrons in six (valence) molecular orbitals (6 e^- /6 MO). The numbers of the CSFs for the four states were 56 (\tilde{X}^1A_1), 51 (\tilde{a}^3B_1), 39 (\tilde{A}^1B_1), and 56 (\tilde{B}^1A_1), respectively. The second active space chosen, CAS II, comprised the first active space with the addition of the $6a_1$, $3b_1$, and $3b_2$ virtual (Rydberg) orbitals, resulting in a six electron/nine molecular orbital (6 e^- /9 MO) active space. The importance of these virtual orbitals was seen in their orbital energies as expressed in the SCF and TCSCF wave functions when diffuse functions were incorporated into the basis set. Using this active space, the numbers of the CSFs for the four states were 684 (\tilde{X}^1A_1), 864 (\tilde{a}^3B_1), 608 (\tilde{A}^1B_1), and 684 (\tilde{B}^1A_1), respectively. In order to construct a CASSCF wave function for the \tilde{B}^1A_1 state, the molecular orbitals were optimized following the second root of the CASSCF Hamiltonian matrix.

Two second-order (SO) CI wave functions were constructed.⁶⁵ The first, CAS I SOCI, included all single and double excitations out of the CAS I references. With the largest basis set [TZ3P(2f,2d)+2diff], the numbers of CSFs for the CAS I SOCI wave functions in C_{2v} symmetry are 313 480 (\tilde{X}^1A_1), 472 296 (\tilde{a}^3B_1), 299 588 (\tilde{A}^1B_1), and 313 480 (\tilde{B}^1A_1), respectively. The second, CAS II SOCI, wave functions were constructed from single and double excitations from the CAS II references. With the TZ3P(2f,2d)+2diff basis set, the numbers of CSFs for the CAS II SOCI wave functions in C_{2v} symmetry are 1 648 704 (\tilde{X}^1A_1), 2 655 766 (\tilde{a}^3B_1), 1 613 948 (\tilde{A}^1B_1), and 1 648 704 (\tilde{B}^1A_1), respectively.

IV. Results and Discussion

It has been found in this study that all four low-lying states of the PH_2^+ molecule have bent equilibrium structures with C_{2v} symmetry. Table 1 contains total energies, equilibrium geometries, dipole moments, harmonic vibrational frequencies with their associated IR intensities, and zero-point energies for the ground state (\tilde{X}^1A_1) predicted at 16 levels of theory for a TCSCF reference. Tables 2 and 3 contain the predicted total energies and geometrical parameters of the first (\tilde{a}^3B_1) and second (\tilde{A}^1B_1) excited states, respectively. The corresponding quantities of the third excited state (\tilde{B}^1A_1) are given in Table 4 for the TCSCF reference. The dipole moments of the PH_2^+ ion were determined with respect to the center of mass. Tables 5 and 6 contain the total energies for all four electronic states in kcal/mol for the CAS I and CAS I SOCI, CAS II and CAS II SOCI levels of theory, respectively. Table 7 contains the relative energies of the first three excited states with respect to the ground state at the SCF, TCSCF, CAS I, and CAS II levels of theory. Table 8 contains the same information at the CISD, CAS I SOCI, and CAS II SOCI levels of theory. In Tables 7 and 8, the zero-point vibrational energy (ZPVE) corrected energy separations (T_0 values) were determined using the CISD harmonic vibrational frequencies with the same basis set.

TABLE 1: Two-Reference Configuration Theoretical Predictions of the Total Energy (in hartrees, Subtract 340), Bond Length (in Å), Bond Angle (in degrees), Dipole Moment (in debye), Harmonic Vibrational Frequencies (in cm^{-1}), Infrared Intensities (in Parentheses in km/mol), and Zero-Point Vibrational Energy (ZPVE in kcal/mol) for the \tilde{X}^1A_1 Ground State of the PH_2^+ Molecule

level of theory	energy	r_e	θ_e	μ_e	$\omega_1(a_1)$	$\omega_2(a_1)$	$\omega_3(b_2)$	ZPVE
TZ2P TCSCF	-1.562 932	1.4060	94.85	1.0583	2538 (1.1)	1231 (7.4)	2545 (0.2)	9.026
TZ2P+diff TCSCF	-1.563 146	1.4059	94.83	1.0634	2539 (1.2)	1230 (8.9)	2545 (0.3)	9.026
TZ3P TCSCF	-1.564 685	1.4052	94.89	1.0210	2566 (1.1)	1234 (7.4)	2573 (0.4)	9.111
TZ3P+2diff TCSCF	-1.564 769	1.4052	94.89	1.0228	2566 (1.1)	1234 (7.7)	2572 (0.4)	9.110
TZ2P(f,d) TCSCF	-1.565 500	1.4060	95.23	1.0724	2561 (0.9)	1230 (9.2)	2567 (0.3)	9.089
TZ2P(f,d)+diff TCSCF	-1.565 717	1.4060	95.22	1.0781	2561 (1.0)	1230 (10.8)	2567 (0.4)	9.090
TZ3P(2f,2d) TCSCF	-1.566 772	1.4048	95.25	1.0469	2562 (0.8)	1231 (9.1)	2569 (0.3)	9.094
TZ3P(2f,2d)+2diff TCSCF	-1.566 885	1.4048	95.26	1.0488	2563 (0.8)	1231 (9.4)	2569 (0.3)	9.097
TZ2P TC-CISD	-1.671 784	1.4181	92.72	1.0424	2404 (0.9)	1155 (5.7)	2410 (0.4)	8.534
TZ2P+diff TC-CISD	-1.672 070	1.4180	92.67	1.0462	2404 (1.0)	1155 (6.9)	2409 (0.5)	8.532
TZ3P TC-CISD	-1.674 464	1.4152	92.93	0.9866	2449 (0.9)	1169 (5.4)	2456 (0.7)	8.684
TZ3P+2diff TC-CISD	-1.674 682	1.4152	92.91	0.9897	2448 (0.9)	1168 (5.7)	2455 (0.7)	8.681
TZ2P(f,d) TC-CISD	-1.688 123	1.4178	93.06	1.0990	2443 (1.7)	1151 (6.2)	2451 (1.2)	8.642
TZ2P(f,d)+diff TC-CISD	-1.688 332	1.4177	93.03	1.1029	2444 (1.7)	1151 (7.3)	2451 (1.3)	8.643
TZ3P(2f,2d) TC-CISD	-1.692 026	1.4150	93.04	1.0544	2456 (1.5)	1155 (5.6)	2466 (1.3)	8.689
TZ3P(2f,2d)+2diff TC-CISD	-1.692 156	1.4150	93.05	1.0559	2457 (1.5)	1155 (5.8)	2467 (1.3)	8.690
experimental fundamental ³¹								~1200

TABLE 2: Theoretical Predictions of the Total Energy (in hartrees, Subtract 340), Bond Length (in Å), Bond Angle (in degrees), Dipole Moment (in debye), Harmonic Vibrational Frequencies (in cm^{-1}), Infrared Intensities (in Parentheses in km/mol), and Zero-Point Vibrational Energy (ZPVE in kcal/mol) for the \tilde{a}^3B_1 State of the PH_2^+ Molecule

level of theory	energy	r_e	θ_e	μ_e	$\omega_1(a_1)$	$\omega_2(a_1)$	$\omega_3(b_2)$	ZPVE
TZ2P SCF	-1.535 715	1.3931	120.87	0.5730	2542 (37.1)	1078 (4.9)	2614 (104.7)	8.911
TZ2P+diff SCF	-1.535 869	1.3930	120.89	0.5822	2542 (36.8)	1077 (5.4)	2614 (105.7)	8.911
TZ3P SCF	-1.537 260	1.3927	120.81	0.5931	2568 (35.1)	1079 (4.8)	2639 (103.0)	8.987
TZ3P+2diff SCF	-1.537 322	1.3927	120.82	0.5949	2568 (35.0)	1079 (4.9)	2639 (103.5)	8.986
TZ2P(f,d) SCF	-1.537 402	1.3936	120.88	0.5754	2559 (36.8)	1075 (4.8)	2631 (104.9)	8.958
TZ2P(f,d)+diff SCF	-1.537 569	1.3936	120.89	0.5844	2559 (36.5)	1075 (5.2)	2631 (105.7)	8.957
TZ3P(2f,2d) SCF	-1.538 410	1.3925	120.84	0.5937	2563 (34.6)	1077 (4.7)	2634 (101.9)	8.969
TZ3P(2f,2d)+2diff SCF	-1.538 523	1.3925	120.84	0.5956	2564 (34.5)	1077 (4.8)	2635 (102.1)	8.972
TZ2P CISD	-1.644 897	1.4047	121.93	0.6506	2406 (40.3)	995 (1.4)	2481 (125.3)	8.409
TZ2P+diff CISD	-1.645 094	1.4047	121.93	0.6587	2406 (39.9)	994 (1.6)	2481 (126.2)	8.407
TZ3P CISD	-1.647 173	1.4028	121.66	0.6355	2446 (37.6)	994 (1.5)	2524 (121.9)	8.527
TZ3P+2diff CISD	-1.647 360	1.4029	121.66	0.6382	2445 (37.7)	994 (1.6)	2522 (122.6)	8.522
TZ2P(f,d) CISD	-1.659 611	1.4056	121.77	0.6670	2436 (43.5)	991 (1.1)	2512 (131.3)	8.490
TZ2P(f,d)+diff CISD	-1.659 763	1.4056	121.78	0.6746	2436 (43.2)	991 (1.2)	2511 (132.0)	8.490
TZ3P(2f,2d) CISD	-1.662 969	1.4033	121.68	0.6514	2451 (40.2)	997 (1.2)	2527 (126.8)	8.542
TZ3P(2f,2d)+2diff CISD	-1.663 093	1.4032	121.67	0.6533	2452 (40.1)	997 (1.2)	2528 (127.1)	8.544

TABLE 3: Theoretical Predictions of the Total Energy (in hartrees, Subtract 340), Bond Length (in Å), Bond Angle (in degrees), Dipole Moment (in debye), Harmonic Vibrational Frequencies (in cm^{-1}), Infrared Intensities (in Parentheses in km/mol), and Zero-Point Vibrational Energy (ZPVE in kcal/mol) for the \tilde{A}^1B_1 State of the PH_2^+ Molecule

level of theory	energy	r_e	θ_e	μ_e	$\omega_1(a_1)$	$\omega_2(a_1)$	$\omega_3(b_2)$	ZPVE
TZ2P SCF	-1.474 156	1.4014	125.85	0.6536	2457 (60.7)	1032 (0.5)	2540 (184.9)	8.619
TZ2P+diff SCF	-1.474 266	1.4014	125.87	0.6619	2457 (60.2)	1031 (0.7)	2540 (186.2)	8.618
TZ3P SCF	-1.475 878	1.4009	125.77	0.6079	2484 (57.6)	1033 (1.0)	2567 (183.0)	8.697
TZ3P+2diff SCF	-1.475 947	1.4009	125.76	0.6125	2484 (57.9)	1032 (1.0)	2566 (183.6)	8.695
TZ2P(f,d) SCF	-1.477 831	1.4014	126.22	0.7052	2477 (58.5)	1028 (0.5)	2561 (194.7)	8.673
TZ2P(f,d)+diff SCF	-1.477 943	1.4015	126.25	0.7130	2477 (58.0)	1028 (0.6)	2561 (195.9)	8.672
TZ3P(2f,2d) SCF	-1.479 179	1.4004	126.23	0.6748	2482 (54.9)	1030 (1.0)	2565 (192.0)	8.688
TZ3P(2f,2d)+2diff SCF	-1.479 269	1.4004	126.22	0.6775	2483 (55.0)	1030 (1.1)	2566 (192.3)	8.689
TZ2P CISD	-1.594 851	1.4200	124.47	0.7530	2274 (49.3)	968 (0.0)	2338 (174.1)	7.976
TZ2P+diff CISD	-1.595 030	1.4200	124.49	0.7607	2273 (48.9)	967 (0.0)	2336 (175.4)	7.972
TZ3P CISD	-1.597 283	1.4182	124.23	0.6936	2314 (48.0)	966 (0.0)	2377 (173.7)	8.086
TZ3P+2diff CISD	-1.597 500	1.4183	124.22	0.6996	2312 (48.4)	964 (0.0)	2376 (174.6)	8.080
TZ2P(f,d) CISD	-1.612 473	1.4194	124.84	0.8008	2315 (53.1)	959 (0.1)	2381 (192.6)	8.085
TZ2P(f,d)+diff CISD	-1.612 595	1.4194	124.85	0.8079	2315 (52.8)	959 (0.1)	2381 (193.7)	8.084
TZ3P(2f,2d) CISD	-1.616 314	1.4172	124.75	0.7479	2331 (50.2)	965 (0.0)	2397 (187.9)	8.139
TZ3P(2f,2d)+2diff CISD	-1.616 424	1.4172	124.74	0.7507	2331 (50.3)	965 (0.0)	2397 (188.2)	8.139

A. Geometries. Regarding theoretical geometries, it is important to recognize the trends imposed by both the size of the basis set used as well as the level of correlation achieved. Larger basis sets tend to contract bonds, while more complete treatments of electron correlation tend to lengthen bonds.^{66–68} While the use of the TZ3P(2f,2d)+2diff basis in conjunction with the CISD method may underestimate bond lengths and

bond angles, it is important to examine the trends in basis set size. The use of larger basis sets becomes necessary in the CASSCF–SOC procedures to determine if theoretically predicted energetic separations between states are convergent and reliable.

At the TZ3P(2f,2d)+2diff TCSCF-CISD level of theory, the bond length (r_e) of the \tilde{X}^1A_1 state of PH_2^+ was predicted to be

TABLE 4: Two Reference Configuration Theoretical Predictions of the Total Energy (in hartrees, Subtract 340), Bond Length (in Å), Bond Angle (in degrees), Dipole Moment (in debye), Harmonic Vibrational Frequencies (in cm^{-1}), Infrared Intensities (in Parentheses in km/mol), and Zero-Point Vibrational Energy (ZPVE in $kcal/mol$) for the \tilde{B}^1A_1 State of the PH_2^+ Molecule

level of theory	energy	r_e	θ_e	μ_e	$\omega_1(a_1)$	$\omega_2(a_1)$	$\omega_3(b_2)$	ZPVE
TZ2P TCSCF	-1.395 011	1.4002	159.10	0.3538	2445 (22.8)	1032 (3.4)	2555 (616.8)	8.624
TZ2P+diff TCSCF	-1.395 076	1.4001	159.10	0.3563	2445 (22.5)	1033 (3.8)	2555 (618.8)	8.624
TZ3P TCSCF	-1.395 951	1.3997	158.90	0.3213	2464 (20.1)	1033 (3.0)	2578 (582.3)	8.684
TZ3P+2diff TCSCF	-1.395 999	1.3997	158.89	0.3276	2463 (20.3)	1034 (3.2)	2578 (583.0)	8.685
TZ2P(f,d) TCSCF	-1.397 430	1.4011	158.40	0.3727	2454 (25.1)	1037 (3.1)	2570 (612.2)	8.665
TZ2P(f,d)+diff TCSCF	-1.397 497	1.4012	158.39	0.3754	2454 (24.4)	1037 (3.4)	2569 (613.4)	8.664
TZ3P(2f,2d) TCSCF	-1.398 239	1.4007	158.12	0.3411	2455 (21.7)	1040 (3.0)	2569 (583.5)	8.668
TZ3P(2f,2d)+2diff TCSCF	-1.398 296	1.4007	158.11	0.3433	2455 (21.6)	1040 (3.2)	2569 (583.8)	8.669
TZ2P TC-CISD	-1.530 565	1.4121	159.63	0.3420	2304 (19.8)	1069 (2.1)	2427 (529.4)	8.291
TZ2P+diff TC-CISD	-1.530 736	1.4121	159.65	0.3429	2303 (19.6)	1069 (2.4)	2427 (531.4)	8.290
TZ3P TC-CISD	-1.532 365	1.4101	159.49	0.3020	2334 (17.7)	1063 (1.6)	2469 (501.7)	8.386
TZ3P+2diff TC-CISD	-1.532 568	1.4102	159.47	0.3081	2333 (17.9)	1065 (1.8)	2468 (502.5)	8.385
TZ2P(f,d) TC-CISD	1.548 911	1.4118	159.62	0.3630	2338 (21.3)	1056 (1.8)	2467 (550.7)	8.379
TZ2P(f,d)+diff TC-CISD	-1.549 008	1.4119	159.63	0.3648	2338 (21.0)	1056 (2.1)	2466 (551.9)	8.378
TZ3P(2f,2d) TC-CISD	-1.552 094	1.4110	159.25	0.3216	2340 (18.6)	1059 (1.8)	2470 (523.2)	8.392
TZ3P(2f,2d)+2diff TC-CISD	-1.552 175	1.4110	159.25	0.3235	2340 (18.7)	1060 (2.0)	2470 (523.4)	8.390

TABLE 5: Total CASSCF (CAS I, 6 e⁻/6 MO) and CASSCF SOCI Energies (in hartrees, Subtract 340) at the CISD Optimized Geometries for Several Electronic States of PH_2^+

level of theory	\tilde{X}^1A_1 TCSCF ^a	\tilde{a}^3B_1 SCF ^a	\tilde{A}^1B_1 SCF ^a	\tilde{B}^1A_1 TCSCF ^a
TZ2P CAS I	-1.595 628	-1.569 571	-1.519 816	-1.444 576
TZ2P+diff CAS I	-1.595 827	-1.569 707	-1.519 929	-1.444 650
TZ3P CAS I	-1.597 134	-1.570 873	-1.521 321	-1.445 530
TZ3P+2diff CAS I	-1.597 218	-1.570 942	-1.521 413	-1.445 613
TZ2P(f,d) CAS I	-1.598 052	-1.571 182	-1.524 099	-1.447 373
TZ2P(f,d)+diff CAS I	-1.598 250	-1.571 331	-1.524 219	-1.447 456
TZ3P(2f,2d) CAS I	-1.599 283	-1.572 177	-1.525 399	-1.448 307
TZ3P(2f,2d)+2diff CAS I	-1.599 391	-1.572 285	-1.525 498	-1.448 369
TZ2P CAS I SOCI	-1.675 662	-1.649 604	-1.600 868	-1.538 044
TZ2P+diff CAS I SOCI	-1.675 948	-1.649 798	-1.601 047	-1.538 228
TZ3P CAS I SOCI	-1.678 340	-1.651 901	-1.603 348	-1.540 014
TZ3P+2diff CAS I SOCI	-1.678 564	-1.652 095	-1.603 574	-1.540 229
TZ2P(f,d) CAS I SOCI	-1.692 431	-1.665 013	-1.619 250	-1.557 359
TZ2P(f,d)+diff CAS I SOCI	-1.692 638	-1.665 162	-1.619 373	-1.557 467
TZ3P(2f,2d) CAS I SOCI	-1.696 415	1.668 488	-1.623 236	-1.560 819
TZ3P(2f,2d)+2diff CAS I SOCI	-1.696 545	-1.668 611	-1.623 347	-1.560 903

^a Reference wave function.**TABLE 6: Total CASSCF (CAS II, 6 e⁻/9 MO) and CASSCF SOCI Energies (in hartrees, Subtract 340) at the CISD Optimized Geometries for Several Electronic States of PH_2^+**

level of theory	\tilde{X}^1A_1 TCSCF ^a	\tilde{a}^3B_1 SCF ^a	\tilde{A}^1B_1 SCF ^a	\tilde{B}^1A_1 TCSCF ^a
TZ2P CAS II	-1.625 736	-1.595 984	-1.543 061	-1.477 367
TZ2P+diff CAS II	-1.625 927	-1.596 112	-1.543 170	-1.477 461
TZ3P CAS II	-1.627 257	-1.597 180	-1.544 437	-1.477 764
TZ3P+2diff CAS II	-1.627 345	-1.597 248	-1.544 526	-1.477 861
TZ2P(f,d) CAS II	-1.628 958	-1.599 190	-1.549 268	-1.480 110
TZ2P(f,d)+diff CAS II	-1.629 143	-1.599 334	-1.549 381	-1.480 205
TZ3P(2f,2d) CAS II	-1.630 411	-1.600 229	-1.550 632	-1.480 769
TZ3P(2f,2d)+2diff CAS II	-1.630 521	-1.600 343	-1.550 730	-1.480 840
TZ2P CAS II SOCI	-1.677 646	-1.651 194	-1.602 355	-1.539 725
TZ2P+diff CAS II SOCI	-1.677 935	-1.651 389	-1.602 537	-1.539 911
TZ3P CAS II SOCI	-1.680 348	-1.653 494	-1.604 838	-1.541 764
TZ3P+2diff CAS II SOCI	-1.680 577	-1.653 692	-1.605 069	-1.541 983
TZ2P(f,d) CAS II SOCI	-1.695 054	-1.667 107	-1.621 217	-1.559 614
TZ2P(f,d)+diff CAS II SOCI	-1.695 262	-1.667 256	-1.621 340	-1.559 723
TZ3P(2f,2d) CAS II SOCI	-1.699 156	-1.670 659	-1.625 279	-1.563 187
TZ3P(2f,2d)+2diff CAS II SOCI	-1.699 286	-1.670 783	-1.625 391	-1.563 272

^a Reference ave function.

1.415 Å, and the bond angle is predicted to be 93.1°—a value that is significantly smaller (by 15°) than that predicted for the \tilde{a}^1A_1 NH_2^+ molecule at the same level of theory.⁴¹ The single-reference predictions for these properties were an r_e value of 1.412 Å and a θ_e value of 92.7°. Adding nondynamical correlation to the ground state in the form of an additional configuration served to slightly increase the bond length and widen the bond angle. The difference in the magnitude of the bond angle in NH_2^+ and PH_2^+ may be qualitatively explained by

the reduced ability of P orbitals (3s and 3p) to hybridize. Balasubramanian predicted¹⁸ in his CASSCF–SOCI study the bond length to be 1.426 Å and the bond angle to be 92.6°. Bauer et al., in their CASSCF–MRCI potential energy function study,⁴⁰ predicted an r_e of 1.423 Å and a θ_e of 92.9°. From these comparisons, it is possible to see that additional excitations in the CI space tend to significantly increase r_e ; however, the inclusion of additional correlation has little effect on the bond angle. Due to the lack of experimental data on the geometries

TABLE 7: Relative Energies T_e (in kcal/mol, T_0 Value in Parentheses) Using SCF, TCSCF, and CASSCF (CAS I and CAS II) Methods for Several Electronic States of the PH_2^+ Molecule

level of theory	\tilde{X}^1A_1 TCSCF ^a	\tilde{a}^3B_1 SCF ^a	\tilde{A}^1B_1 SCF ^a	\tilde{B}^1A_1 TCSCF ^a
TZ2P (TC)SCF	0.0	17.079 (16.964)	55.708 (55.301)	105.372 (104.970)
TZ2P+diff (TC)SCF	0.0	17.117 (17.002)	55.773 (55.365)	105.466 (105.064)
TZ3P (TC)SCF	0.0	17.209 (17.085)	55.727 (55.313)	105.882 (105.455)
TZ3P+2diff (TC)SCF	0.0	17.223 (17.099)	55.737 (55.322)	105.905 (105.480)
TZ2P(f,d) (TC)SCF	0.0	17.632 (17.501)	55.013 (54.597)	105.466 (105.042)
TZ2P(f,d)+diff (TC)SCF	0.0	17.663 (17.530)	55.079 (54.661)	105.560 (105.134)
TZ3P(2f,2d) (TC)SCF	0.0	17.797 (17.672)	54.965 (54.559)	105.756 (105.330)
TZ3P(2f,2d)+2diff (TC)SCF	0.0	17.797 (17.672)	54.980 (54.572)	105.791 (105.363)
TZ2P CAS I	0.0	16.351 (16.226)	47.573 (47.015)	94.787 (94.544)
TZ2P+diff CAS I	0.0	16.391 (16.266)	47.627 (47.067)	94.865 (94.623)
TZ3P CAS I	0.0	16.479 (16.322)	47.573 (46.975)	95.133 (94.835)
TZ3P+2diff CAS I	0.0	16.488 (16.329)	47.568 (46.967)	95.134 (94.838)
TZ2P(f,d) CAS I	0.0	16.861 (16.709)	46.406 (45.849)	94.553 (94.290)
TZ2P(f,d)+diff CAS I	0.0	16.892 (16.739)	46.455 (45.896)	94.625 (94.360)
TZ3P(2f,2d) CAS I	0.0	17.009 (16.862)	46.363 (45.813)	94.739 (94.442)
TZ3P(2f,2d)+2diff CAS I	0.0	17.009 (16.863)	46.369 (45.818)	94.768 (94.468)
TZ2P CAS II	0.0	18.670 (18.545)	51.879 (51.321)	93.103 (92.860)
TZ2P+diff CAS II	0.0	18.709 (18.584)	51.931 (51.371)	93.164 (92.922)
TZ3P CAS II	0.0	18.874 (18.717)	51.970 (51.372)	93.808 (93.510)
TZ3P+2diff CAS II	0.0	18.886 (18.727)	51.970 (51.369)	93.803 (93.507)
TZ2P(f,d) CAS II	0.0	18.680 (18.528)	50.006 (49.449)	93.404 (93.141)
TZ2P(f,d)+diff CAS II	0.0	18.705 (18.552)	50.051 (49.492)	93.460 (93.195)
TZ3P(2f,2d) CAS II	0.0	18.940 (18.793)	50.062 (49.512)	93.902 (93.605)
TZ3P(2f,2d)+2diff CAS II	0.0	18.937 (18.791)	50.070 (49.519)	93.926 (93.626)
experimental ³³	0.0	(16.1–18.4)	(~44.3)	

^a Reference wave function.**TABLE 8: Relative Energies T_e (in kcal/mol, T_0 Value in Parentheses) Using CISD and CASSCF MRCI (CAS I MRCI I and CAS II MRCI II) Methods for Several Electronic States of the PH_2^+ Molecule**

level of theory	\tilde{X}^1A_1 TCSCF ^a	\tilde{a}^3B_1 SCF ^a	\tilde{A}^1B_1 SCF ^a	\tilde{B}^1A_1 TCSCF ^a
TZ2P CISD	0.0	16.872 (16.747)	48.276 (47.718)	88.616 (88.373)
TZ2P+diff CISD	0.0	16.928 (16.803)	48.343 (47.783)	88.688 (88.446)
TZ3P CISD	0.0	17.125 (16.968)	48.432 (47.834)	89.169 (88.871)
TZ3P+2diff CISD	0.0	17.145 (16.986)	48.432 (47.831)	89.178 (88.882)
TZ2P(f,d) CISD	0.0	17.892 (17.740)	47.471 (46.914)	87.357 (87.094)
TZ2P(f,d)+diff CISD	0.0	17.927 (17.774)	47.526 (46.967)	87.427 (87.162)
TZ3P(2f,2d) CISD	0.0	18.234 (18.087)	47.510 (46.960)	87.809 (87.512)
TZ3P(2f,2d)+2diff CISD	0.0	18.237 (18.091)	47.523 (46.972)	87.839 (87.539)
TZ2P CAS I SOCI	0.0	16.352 (16.227)	46.934 (46.376)	86.357 (86.114)
TZ2P+diff CAS I SOCI	0.0	16.409 (16.284)	47.001 (46.441)	86.421 (86.179)
TZ3P CAS I SOCI	0.0	16.591 (16.434)	47.058 (46.460)	86.801 (86.503)
TZ3P+2diff CAS I SOCI	0.0	16.610 (16.451)	47.057 (46.456)	86.807 (86.511)
TZ2P(f,d) CAS I SOCI	0.0	17.205 (17.053)	45.922 (45.365)	84.759 (84.496)
TZ2P(f,d)+diff CAS I SOCI	0.0	17.241 (17.088)	45.975 (45.416)	84.821 (84.556)
TZ3P(2f,2d) CAS I SOCI	0.0	17.524 (17.377)	45.921 (45.371)	85.088 (84.791)
TZ3P(2f,2d)+2diff CAS I SOCI	0.0	17.529 (17.383)	45.932 (45.381)	85.117 (84.817)
TZ2P CAS II SOCI	0.0	16.599 (16.474)	47.246 (46.688)	86.547 (86.304)
TZ2P+diff CAS II SOCI	0.0	16.658 (16.533)	47.313 (46.753)	86.611 (86.369)
TZ3P CAS II SOCI	0.0	16.851 (16.694)	47.383 (46.785)	86.963 (86.665)
TZ3P+2diff CAS II SOCI	0.0	16.871 (16.712)	47.382 (46.781)	86.969 (86.673)
TZ2P(f,d) CAS II SOCI	0.0	17.537 (17.385)	46.333 (45.776)	84.990 (84.727)
TZ2P(f,d)+diff CAS II SOCI	0.0	17.574 (17.421)	46.387 (45.828)	85.052 (84.787)
TZ3P(2f,2d) CAS II SOCI	0.0	17.882 (17.735)	46.359 (45.809)	85.322 (85.025)
TZ3P(2f,2d)+2diff CAS II SOCI	0.0	17.886 (17.740)	46.370 (45.819)	85.350 (85.050)
experimental ³³	0.0	(16.1–18.4)	(~44.3)	

of any of the electronic states of PH_2^+ , it is difficult to quantify the quality of these predictions. It is reasonable to expect, though, that at the largest basis CISD level, the bond lengths found in this research are slightly underestimated.

The bond length of the \tilde{a}^3B_1 state is predicted to be 1.403 Å, and the bond angle lies at 121.7°. This bond angle is approximately 32° smaller than that of the \tilde{X}^3B_1 state of NH_2^+ .⁴¹ Again, Balasubramanian¹⁸ arrived at a longer r_e of 1.416 Å. However, our θ_e value is in good agreement with his prediction of 121.8°, showing that there is little change in bond angle when correlation above the CISD level is included.

The bond length of the \tilde{A}^1B_1 state is predicted to be 1.417

Å, and the bond angle lies at 124.7°. The bond length and bond angle predicted by Balasubramanian were 1.431 Å and 124.0°, respectively. The predicted θ_e is significantly smaller (by 38°) than that of the \tilde{b}^1B_1 state of NH_2^+ .⁴¹ The corresponding values arrived at by Bauer et al. were $r_e = 1.427$ Å and $\theta_e = 124.5^\circ$. Here we see the same trends in bond length as we saw above; however, now it appears that correlation has a larger affect on the bond angle, as evidenced by the larger difference between the angle predicted by the previous multireference CI methods and that predicted in this study.

The bond length of the \tilde{B}^1A_1 state is predicted to be 1.411 Å, and the bond angle lies at 159.3°. On the basis of the above

trends, accepting the geometry predictions of Bauer et al. and Balasubramanian, we can reasonably expect the bond length to be $\sim 1\%$ longer and the bond angle to be, at most, in error by 0.5%. In the second 1A_1 state of CH_2 , the anharmonicity of the bending potential (because the barrier to linearity is only a few cm^{-1}) necessitates the use of high levels of correlation to accurately approach the full CI values for θ_e as well as the symmetric bending frequency.^{4,12,69,70} In the \tilde{B}^1A_1 state of PH_2^+ , on the other hand, whose bond angle is much smaller (by $\sim 12^\circ$) than that of \tilde{c}^1A_1 CH_2 , it is more reasonable to assume that the CISD predictions for both θ_e and the symmetric bending frequency are fairly reliable. We estimate the barrier to linearity to be approximately 2.5 kcal/mol (880 cm^{-1}) based on TZ2P CISD calculations of the equilibrium geometries of both linear $\tilde{B}^1\Sigma_g^+$ PH_2^+ and bent \tilde{B}^1A_1 PH_2^+ . Therefore, while the frequency for bending in the state is still larger than the barrier to linearity, the situation is much improved over that of the \tilde{c} state of CH_2 . Another interesting observation is the fact that the equilibrium geometry of the \tilde{B}^1A_1 state is not linear like its second-row analogue, $\tilde{c}^1\Sigma_g^+$ NH_2^+ .⁴¹ If we consider the \tilde{B}^1A_1 state a double excitation from the \tilde{X}^1A_1 state, then the orbital which most affects the geometry (according to the Walsh diagram for AH_2 molecules) would be the $2b_2$, which prefers a linear geometry. But because of the decreased ability of the P orbitals to participate in sp-mixing (relative to N), this orbital may not be as influential, and the molecule remains bent.

The ordering of the bond lengths is slightly different here than in methylene's case.^{4,12} For CH_2 at the same level of theory as presented here, the ordering was found to be (r_e values in Å)

$$\tilde{a}^1A_1 (1.105) > \tilde{X}^3B_1 (1.075) > \tilde{b}^1B_1 (1.071) > \tilde{c}^1A_1 \quad (1.064)$$

In PH_2^+ , we find that

$$\tilde{A}^1B_1 (1.417) > \tilde{X}^1A_1 (1.415) > \tilde{B}^1A_1 (1.411) > \tilde{a}^3B_1 \quad (1.403)$$

This is a very narrow range indeed, and it seems that the bond length changes little upon electronic excitation. This should, as shown below, have some ramifications on the harmonic vibrational frequencies. Additionally, one should note that with the addition of correlation by the CISD method, the bond length increased by 0.01 Å or less for all four states. The ordering of the bond angles follows as

$$\tilde{B}^1A_1 (159.3) > \tilde{A}^1B_1 (124.7) > \tilde{a}^3B_1 (121.7) > \tilde{X}^1A_1 \quad (93.1)$$

This both follows the ordering in CH_2 ¹² and is an example of Walsh's rules.⁷¹ When the $5a_1$ orbital is doubly occupied as the highest occupied molecular orbital, the molecule is bent (\tilde{X}^1A_1). Single excitations from the $5a_1$ orbital into the $2b_1$ orbital, which is perpendicular to the molecular plane, allow the $2b_2$ orbital to have more influence on the geometry, and the angle widens (\tilde{a}^3B_1 and \tilde{A}^1B_1). Double excitations (\tilde{B}^1A_1) increase the angle further. Also note that electron correlation provided by the CISD method serves to increase the bond angle in the \tilde{a}^3B_1 and \tilde{B}^1A_1 states, while it decreases the bond angle of the \tilde{X}^1A_1 and \tilde{A}^1B_1 states.

B. Dipole Moments. At the TZ3P(2f,2d)+2diff CISD or TC-CISD level of theory, the four electronic states of PH_2^+ had dipole moments (shown in Tables 1–4) with the following magnitudes: 1.056 D (\tilde{X}^1A_1), 0.653 D (\tilde{a}^3B_1), 0.751 D (\tilde{A}^1B_1), and 0.324 D (\tilde{B}^1A_1). They all have the same sign, P^+H^- , as the cation is largely created by removing an electron from the

$2b_1$ orbital (centered on P) from the PH_2 radical. The relatively large dipole moments (which were calculated relative to the center of mass) of these states should make microwave spectroscopic investigations possible, if the cations can be isolated in significant quantities in the gas phase. It should be noted that the dipole moments predicted for the \tilde{B}^1A_1 state are expectation values of the dipole moment operator, while those determined for the other three states are gradient corrected. The \tilde{a}^3B_1 and \tilde{A}^1B_1 dipoles are similar due to the fact that they have very similar geometries and electronic configurations (i.e. they only differ in spin symmetry). The ground state has a much larger dipole due to the additional electron in the $5a_1$ orbital which creates a much smaller ($\sim 30^\circ$ smaller) bond angle than either the \tilde{a}^3B_1 or the \tilde{A}^1B_1 states. The \tilde{B}^1A_1 has a much smaller dipole moment due to its large bond angle of $\sim 160^\circ$, which is attributable to the additional electron in the $2b_1$ orbital. Correlation effects tend to decrease the dipole moment by approximately 0.02 D for the \tilde{B}^1A_1 state, while they tend to increase the dipole of the \tilde{X}^1A_1 , \tilde{a}^3B_1 , and \tilde{A}^1B_1 states by 0.02–0.08 D.

C. Harmonic Vibrational Frequencies. Without experimental data, it is difficult to determine the accuracy of the frequency predictions presented here. However, using the same levels of theory on SiH_2 and CH_2 —two systems for which there are quite a few experimental fundamentals known—Yamaguchi et al.^{12,72} were able to determine that at the TZ3P(2f,2d)+2diff CISD level of theory there is an error of approximately 5% or less between experimental and theoretical vibrational frequencies. Larger errors occur only when anharmonic effects are particularly large.⁴ For PH_2^+ , it is reasonable to assume that anharmonicity should not play as large a role, except in the \tilde{B}^1A_1 state bending potential, as the bond angles and bond lengths are not inordinately wide or long, respectively.

The study by Bauer et al.⁴⁰ is the most reliable source for harmonic vibrational frequencies of the ground and second excited electronic states. Our largest basis CISD predicted harmonic vibrational frequencies for the \tilde{X}^1A_1 state of $\omega_1(a_1) = 2457$ cm^{-1} , $\omega_2(a_1) = 1155$ cm^{-1} , and $\omega_3(b_2) = 2467$ cm^{-1} are within 4% of those of Bauer et al. ($\omega_1(a_1) = 2399$ cm^{-1} , $\omega_2(a_1) = 1113$ cm^{-1} , and $\omega_3(b_2) = 2413$ cm^{-1}).

Our predictions for the vibrational frequencies of the \tilde{a}^3B_1 state are $\omega_1(a_1) = 2452$ cm^{-1} , $\omega_2(a_1) = 997$ cm^{-1} , and $\omega_3(b_2) = 2528$ cm^{-1} . The only other published frequencies for this particular state were by Berkowitz et al.,³² who added theoretical harmonic vibrational frequencies at the HF/6-31G* level to help interpret their photoionization spectra of PH_2^+ (PH_2). Naturally, at the HF level, the frequencies were quite a bit higher.

Our predictions for the vibrational frequencies of the \tilde{A}^1B_1 state are $\omega_1(a_1) = 2331$ cm^{-1} , $\omega_2(a_1) = 965$ cm^{-1} , and $\omega_3(b_2) = 2397$ cm^{-1} . These values are within 5.5% of those of Bauer et al. ($\omega_1(a_1) = 2259$ cm^{-1} , $\omega_2(a_1) = 914$ cm^{-1} , and $\omega_3(b_2) = 2292$ cm^{-1}).

At the largest basis CISD level of theory, PH_2^+ symmetric stretching ($\omega_1(a_1)$) frequencies (in cm^{-1}) are in the order of

$$\tilde{X}^1A_1 (2457) > \tilde{a}^3B_1 (2452) > \tilde{B}^1A_1 (2340) > \tilde{A}^1B_1 \quad (2331)$$

while the ordering of the asymmetric stretching ($\omega_3(b_2)$) frequencies is

$$\tilde{a}^3B_1 (2528) > \tilde{B}^1A_1 (2470) > \tilde{X}^1A_1 (2467) > \tilde{A}^1B_1 \quad (2397)$$

The orderings of $\omega_3(b_2)$ are in line with Badger's prediction^{73,74} that the larger vibrational frequency can be associated with the

shorter bond length. The \tilde{X}^1A_1 symmetric stretching frequency does not follow this notion; however, as stated above, the range of bond lengths is very narrow; thus it is possible that there may be some imperfections in the ordering of the frequencies. The bending mode ($\omega_2(a_1)$) shows the following ordering

$$\tilde{X}^1A_1 (1155) > \tilde{B}^1A_1 (1060) > \tilde{a}^3B_1 (997) > \tilde{A}^1B_1 (965)$$

Here we see the $\omega_2(a_1)$ of the \tilde{B}^1A_1 state (whose bond angle is much greater than the other three) is out of order according to the usual expectation that smaller bond angles lead to larger vibrational frequencies. This is not too unusual, as bending modes do not always follow the same trends as stretching frequencies. The experimental bending fundamental³¹ estimated from Edwards' et al. laser photodissociation of PH_2^+ is most likely given a value that is too high.

D. Infrared (IR) Intensities. All three of the vibrational IR intensities of the ground state (\tilde{X}^1A_1) of PH_2^+ are rather small, and it would be very difficult to obtain the IR spectrum of this species even if it could be produced in significant amounts. On the other hand, the intensities of the $\omega_1(a_1)$ and $\omega_3(b_2)$ modes of the \tilde{a}^3B_1 state are relatively large. Even though the $\tilde{a}^3B_1 \leftarrow \tilde{X}^1A_1$ transition is electronically forbidden, an IR spectrum of the \tilde{a}^3B_1 state should be obtained if it is produced in sufficient quantity. While the IR intensity of the bending mode of $\tilde{A}^1B_1 PH_2^+$ is very weak, the symmetric and asymmetric stretching modes have large intensities, and should be rather easy to detect by IR techniques. Both the symmetric stretching and the bending frequencies have low intensities, leaving only the asymmetric frequency (whose IR intensity is predicted to be very large) of the \tilde{B}^1A_1 electronic state probable for IR investigation.

E. Energetics. 1. $\tilde{a}^3B_1 \leftarrow \tilde{X}^1A_1$ Separation. The experimental data provided by Berkowitz et al.³³ gives a singlet-triplet splitting (T_0 value) of 16.1–18.4 kcal/mol (0.70–0.80 eV, 5630–6440 cm^{-1}). The extensive geometry optimizations of the ground and first two excited states of PH_2^+ by Balasubramanian¹⁸ at the CASSCF–SOC1 (6 $e^-/6$ MO) level of theory, in principle, should be very accurate. His prediction for the singlet-triplet separation (T_e value) was 17.73 kcal/mol, which falls near the high end of the experimental range. With the largest basis set, nearly all levels of theory employed in this study, with the exception of the CISD and CAS II levels which appear to be overestimating the energy difference, fall within the experimental limits. Surprisingly, the SCF prediction is right in line with Balasubramanian's values. The agreement between the SCF and CASSCF levels of theory and experiment is most likely fortuitous, as these methods have not been shown to accurately predict energy separations. The CAS II SOC1 method predicts a T_e value of 17.89 kcal/mol, which is only a 0.2 kcal/mol difference from Balasubramanian's prediction. In the case of SiH_2 and CH_2 ,^{12,72} the CASSCF–SOC1 energy separations (T_0 , at CISD geometries), were in error from experiment by 0.7 kcal/mol or less. It is reasonable to assume the same error bars on our T_0 prediction of 17.74 kcal/mol (0.77 eV, 6200 cm^{-1}) for the $\tilde{a}^3B_1 \leftarrow \tilde{X}^1A_1$ splitting of the isovalent PH_2^+ molecule. It is also reasonable to assume that the experimental value of 16.1 kcal/mol is probably too low and that a more appropriate lower bound would be 17.0 kcal/mol.

2. $\tilde{A}^1B_1 \leftarrow \tilde{X}^1A_1$ Separation. The experimentally estimated T_0 value of the \tilde{A}^1B_1 state is 44.3 kcal/mol.³³ All levels of theory employed in this study overestimate this value. However, the largest basis set CAS II SOC1 T_e value, 46.37 kcal/mol, is in fair agreement with Balasubramanian's prediction of 45.06 kcal/mol.¹⁸ Bauer et al. predicted a T_e value of 45.49 kcal/

mol. The significant ZPVE difference between the \tilde{X}^1A_1 and \tilde{A}^1B_1 states provides a large correction to the T_e value, and the resulting prediction for T_0 is 45.82 kcal/mol (1.99 eV, 16 030 cm^{-1}). Again, with a similar basis set and level of theory, Yamaguchi et al. were able to estimate the $\tilde{A}^1B_1 \leftarrow \tilde{X}^1A_1$ separation of CH_2 (T_0) within 0.5 kcal/mol of the experimental value. Therefore, this is a reasonable error bar to apply in this case also.

3. $\tilde{B}^1A_1 \leftarrow \tilde{X}^1A_1$ Separation. Correlation has a dramatic effect on the T_e (\tilde{B}^1A_1) value, decreasing it by as much as 20 kcal/mol. At the highest level of theory (CAS II SOC1) the T_0 value for the \tilde{B}^1A_1 state of PH_2^+ is predicted to be 85.05 kcal/mol (3.69 eV, 29 750 cm^{-1}). To our knowledge, this is the first theoretical determination of the $\tilde{B}^1A_1 \leftarrow \tilde{X}^1A_1$ separation, and no experimental values for this quantity exist. In previous studies of the second 1A_1 state of SiH_2 and CH_2 , the estimated error in the T_0 value for these states was found to be ± 1.5 kcal/mol. While there had been no experimental values for these predictions, it was possible to estimate the error based on the CASSCF–SOC1 method's performance on the $\tilde{a}^3B_1 \leftarrow \tilde{X}^1A_1$ and $\tilde{A}^1B_1 \leftarrow \tilde{X}^1A_1$ separations as well as a consideration of the increased error due to the flatter bending potentials of the second 1A_1 state. Due to the similarity between this study and the previous works on related molecules^{12,72} it is possible to give a reliable estimate of the error in our prediction as ± 1.5 kcal/mol (± 525 cm^{-1}).

4. Ionization Potentials. As a further aid to experimentalists searching for the PH_2 cation using, for example, photoelectron spectroscopy, adiabatic and vertical ionization potentials (IP_{ad} and IP_{vert}) were determined at the TZ3P(2f,2d)+2diff CISD level of theory for the $PH_2 \rightarrow PH_2^+ + e^-$ ionization. The \tilde{X}^2B_1 state of PH_2 molecule at this level of theory has an r_e value of 1.413 Å and a θ_e value of 92.21°. The zero-point-corrected first IP_{ad} (i.e. from the \tilde{X}^2B_1 state of PH_2 to the \tilde{X}^1A_1 state of PH_2^+) was found to be 220.3 kcal/mol (9.55 eV, 77 110 cm^{-1}). This is in reasonable agreement with the experimental value of 9.82 eV determined by Berkowitz et al.³³ The predicted value for the first (non ZPVE corrected) IP_{vert} is 220.3 kcal/mol (9.55 eV, 77 110 cm^{-1}). The near equality of the IP_{ad} and IP_{vert} values is a byproduct of the fact that the ground state geometries of both the molecule and the cation are very similar. The next IP_{ad} ($\tilde{a}^3B_1 PH_2^+ \leftarrow \tilde{X}^2B_1 PH_2$) is predicted to lie at 238.4 kcal/mol (10.34 eV, 83 440 cm^{-1}). The experimental value lies between 10.52 and 10.62 eV.³³ The IP_{vert} value for this transition is 250.4 kcal/mol (10.86 eV, 87 640 cm^{-1}). The next IP_{ad} ($\tilde{A}^1B_1 PH_2^+ \leftarrow \tilde{X}^2B_1 PH_2$) is predicted to be 267.8 kcal/mol (11.61 eV, 93 730 cm^{-1}), and the IP_{vert} is 282.1 kcal/mol (12.23 eV, 98 740 cm^{-1}). The final predicted IP_{ad} ($\tilde{B}^1A_1 PH_2^+ \leftarrow \tilde{X}^2B_1 PH_2$) is 307.9 kcal/mol (13.35 eV, 107 800 cm^{-1}), and the IP_{vert} value is 361.2 kcal/mol (15.66 eV, 126 400 cm^{-1}). The increase in differences between vertical and adiabatic ionization potentials reflects the increase in the bond angle of PH_2^+ with electronic excitation.

V. Conclusions

Four low-lying electronic states of PH_2^+ have been systematically investigated. Several high levels of ab initio electronic structure theory have been applied in an effort to provide experimentalists with reliable energetic and spectroscopic parameters. The abundance of information provided herein will also aid theoreticians in making reliable estimates about energetic and geometric characteristics when very high levels of theory cannot be used. All four states are determined to have bent equilibrium structures with C_{2v} symmetry. As in SiH_2 ,⁷² the bond angles of these states are considerably smaller than those of the corresponding states of both CH_2 and NH_2^+ .

TABLE 9: Largest Basis (TC)CISD Geometries for Four Low-Lying Electronic States of CH_2 , NH_2^+ , SiH_2 , and PH_2^+ ^a

molecule	1A_1		3B_1		1B_1		2A_1	
	r_e	θ_e	r_e	θ_e	r_e	θ_e	r_e	θ_e
CH_2^{12}	1.105	102.3	1.075	132.9	1.071	142.9	1.064	171.6
NH_2^{+41}	1.044	108.2	1.027	150.5	1.027	161.4	1.030	180.0
SiH_2^{72}	1.505	92.9	1.469	118.2	1.473	122.9	1.450	160.8
PH_2^+	1.415	93.1	1.403	121.7	1.417	124.7	1.411	159.3

^a Bond lengths are in angstroms, and bond angles are in degrees.

This follows the expectation that hybridization of the A atom orbitals in AH_2 molecules decreases as a group is descended in the periodic table. Table 9 is included as an aid to show this trend. Included are the geometrical parameters predicted for CH_2 ,¹² NH_2^+ ,⁴¹ SiH_2 ,⁷² and PH_2^+ at similar levels of theory.

The T_0 values for the first excited state (\tilde{a}^3B_1), the second excited state (\tilde{A}^1B_1), and the third excited state (\tilde{B}^1A_1) are predicted to be 17.74 kcal/mol (0.77 eV, 6200 cm^{-1}), 45.82 kcal/mol (1.99 eV, 16 030 cm^{-1}), and 85.05 kcal/mol (3.69 eV, 29 750 cm^{-1}), respectively. The error bars for these values are estimated to be ± 0.5 kcal/mol (\tilde{a}^3B_1), ± 0.7 kcal/mol (\tilde{A}^1B_1), and ± 1.5 kcal/mol (\tilde{B}^1A_1), respectively.

Acknowledgment. T.V.H. would like to acknowledge Jeffrey C. Stephens for helpful discussions. This research was supported by the National Science Foundation, Grant CHE-9527468.

References and Notes

- Herzberg, G. *Proc. R. Soc. London Ser. A* **1961**, 262, 291.
- Foster, J. M.; Boys, S. F. *Rev. Mod. Phys.* **1960**, 32, 305.
- Bender, C. F.; Schaefer, H. F. *J. Amer. Chem. Soc.* **1970**, 92, 4984.
- Sherrill, C. D.; Van Huis, T. J.; Yamaguchi, Y.; Schaefer, H. F. *THEOCHEM*, special issue on bench mark computations, in press. See methods and references therein.
- Petek, H.; Nesbitt, D. J.; Moore, C. B.; Birss, F. W.; Ramsay, D. A. *J. Chem. Phys.* **1987**, 86, 1189.
- Duxbury, G.; Jungen, C. *Mol. Phys.* **1988**, 63, 981.
- Jensen, P.; Bunker, P. R. *J. Chem. Phys.* **1988**, 89, 1327.
- Comeau, D. C.; Shavitt, I.; Jensen, P.; Bunker, P. R. *J. Chem. Phys.* **1989**, 90, 6491.
- Petek, H.; Nesbitt, D. J.; Darwin, D. C.; Ogilby, P. R.; Moore, C. B.; Ramsay, D. A. *J. Chem. Phys.* **1989**, 91, 6566.
- Green, W. H.; Handy, N. C.; Knowles, P. J.; Carter, S. *J. Chem. Phys.* **1991**, 94, 118.
- Woon, D. E.; Dunning, T. H. *J. Chem. Phys.* **1995**, 103, 4572.
- Yamaguchi, Y.; Sherrill, C. D.; Schaefer, H. F. *J. Phys. Chem.* **1996**, 100, 7911.
- Shavitt, I. *Tetrahedron* **1985**, 41, 1531.
- Davidson, E. R.; Feller, D.; Phillips, P. *Chem. Phys. Lett.* **1980**, 76, 416.
- Handy, N. C.; Yamaguchi, Y.; Schaefer, H. F. *J. Chem. Phys.* **1986**, 84, 4481.
- Balasubramanian, K.; McLean, A. D. *J. Chem. Phys.* **1986**, 85, 5117.
- Bauschlicher, C. W.; Langhoff, S. R.; Taylor, P. R. *J. Chem. Phys.* **1987**, 87, 387.
- Balasubramanian, K. *Chem. Phys. Lett.* **1993**, 204, 601.
- Balasubramanian, K.; Chung, Y. S.; Glaunsinger, W. S. *J. Chem. Phys.* **1993**, 98, 8859.
- Cramer, C. J.; Dulles, F. J.; Storer, J. W.; Worthington, S. E. *Chem. Phys. Lett.* **1994**, 218, 387.
- Karolczak, J.; Harper, W. W.; Grev, R. S.; Clouthier, D. J. *J. Chem. Phys.* **1995**, 103, 2839.
- Vager, Z.; Naaman, R.; Kanter, E. P. In *Ion and Cluster Ion Spectroscopy and Structure*; Maier, J. P., Ed.; Elsevier Science Publishers B. V.: Amsterdam, The Netherlands, 1989.
- Turner, B. E.; Bally, J. *Astrophys. J. Lett.* **1987**, 87, 321, L75.
- Ziurys, L. M. *Astrophys. J. Lett.* **1987**, 321, L81.
- Ridgeway, S. T.; Wallace, L.; Smith, G. R. *Astrophys. J.* **1976**, 207, 1002.
- Thorne, L. R.; Anicich, V. G.; Huntress, W. T. *Chem. Phys. Lett.* **1983**, 98, 162.
- Smith, D.; McIntosh, B. J.; Adams, N. G. *J. Chem. Phys.* **1989**, 90, 6213.
- Esseffar, M.; Luna, A.; M6, O.; Y6n6ez, M. *Chem. Phys. Lett.* **1994**, 223, 240.

- Parish, M. B. *J. Electrochem. Soc.* **1980**, 127, 2729.
- Berkowitz, J. *J. Chem. Phys.* **1988**, 89, 7065.
- Edwards, C. P.; Jackson, P. A.; MacLean, C. S.; Sarre, P. *J. Bull. Soc. Chim. Belg.* **1983**, 92, 605.
- Berkowitz, J.; Curtiss, L. A.; Gibson, S. T.; Greene, J. P.; Hillhouse, G. L.; Pople, J. A. *J. Chem. Phys.* **1986**, 84, 375.
- Berkowitz, J.; Cho, H. *J. Chem. Phys.* **1989**, 90, 1.
- Ball, J. R.; Thomson, C. *Int. J. Quantum Chem.* **1978**, 14, 39.
- Dyke, J. M.; Jonathan, N.; Morris, A. *Int. Rev. Phys. Chem.* **1982**, 2, 22.
- Pople, J. A.; Curtiss, L. A. *J. Phys. Chem.* **1987**, 91, 3637.
- Dunning, T. H. *J. Chem. Phys.* **1989**, 90, 1007.
- Bruna, P. J.; Peyerimhoff, S. D. *Bull. Soc. Chim. Belg.* **1983**, 92, 525.
- Bruna, P. J.; Hirsch, G.; Bunker, R. J.; Peyerimhoff, S. D. In *Molecular Ions-Geometric and Electronic Structures*; Berkowitz, J., Groenewald, K. O., Eds.; Plenum: New York, 1983; Vol. 90, pp 309–354.
- Bauer, C.; Hirst, D. M.; Batey, A. D.; Sarre, P. J.; Rosmus, P. *J. Chem. Soc., Faraday Trans.* **1995**, 91, 2053.
- Stephens, J. C.; Yamaguchi, Y.; Sherrill, C. D.; Schaefer, H. F. It should be noted that the basis set used in this work was similar in every way except that three sets of Cartesian d- and f-like functions were used (unpublished).
- McLean, A. D.; Chandler, G. S. *J. Chem. Phys.* **1980**, 72, 5639.
- Huzinaga, S. *Approximate Atomic Wavefunctions, Vol. II*; Department of Chemistry: University of Alberta, 1971.
- Dunning, T. H. *J. Chem. Phys.* **1971**, 55, 716.
- Huzinaga, S. *J. Chem. Phys.* **1965**, 42, 1293.
- Lee, T. J.; Schaefer, H. F. *J. Chem. Phys.* **1985**, 83, 1784.
- Pulay, P. *Mol. Phys.* **1969**, 17, 197.
- Pulay, P. In *Modern Theoretical Chemistry*; Schaefer, H. F., Ed.; Plenum Press: New York, 1977; Vol. 4, pp 153–185.
- Yamaguchi, Y.; Osamura, Y.; Goddard, J. D.; Schaefer, H. F. *A New Dimension to Quantum Chemistry: Analytic Derivative Methods in Ab Initio Molecular Electronic Structure Theory*; Oxford University Press: New York, 1994.
- Saxe, P.; Yamaguchi, Y.; Schaefer, H. F. *J. Chem. Phys.* **1982**, 77, 5647.
- Osamura, Y.; Yamaguchi, Y.; Saxe, P.; Vincent, M. A.; Gaw, J. F.; Schaefer, H. F. *J. Chem. Phys.* **1982**, 72, 131.
- Osamura, Y.; Yamaguchi, Y.; Saxe, P.; Fox, D. J.; Vincent, M. A.; Schaefer, H. F. *J. Mol. Struct.* **1983**, 103, 183.
- Yamaguchi, Y.; Frisch, M. J.; Gaw, J. F.; Schaefer, H. F.; Binkley, J. S. *J. Chem. Phys.* **1986**, 84, 2262.
- Yamaguchi, Y.; Osamura, Y.; Schaefer, H. F. *J. Am. Chem. Soc.* **1983**, 105, 7506.
- Yamaguchi, Y.; Frisch, M. J.; Lee, T. J.; Schaefer, H. F.; Binkley, J. S. *Theor. Chim. Acta* **1986**, 69, 337.
- Brooks, B. R.; Laidig, W. D.; Saxe, P.; Goddard, J. D.; Yamaguchi, Y.; Schaefer, H. F. *J. Chem. Phys.* **1980**, 72, 4652.
- Rice, J. E.; Amos, R. D.; Handy, N. C.; Lee, T. J.; Schaefer, H. F. *J. Chem. Phys.* **1986**, 85, 963.
- Lee, T. J.; Allen, W. D.; Schaefer, H. F. *J. Chem. Phys.* **1987**, 87, 7062.
- Allen, W. D.; Schaefer, H. F. *J. Chem. Phys.* **1987**, 87, 7076.
- King, R. A.; Schaefer, H. F. *Spectrochim. Acta*, in press.
- Janssen, C. L.; Seidl, E. T.; Scuseria, G. E.; Hamilton, T. P.; Yamaguchi, Y.; Remington, R. B.; Xie, Y.; Vacek, G.; Sherrill, C. D.; Crawford, T. D.; Fermann, J. T.; Allen, W. D.; Brooks, B. R.; Fitzgerald, G. B.; Fox, D. J.; Gaw, J. F.; Handy, N. C.; Laidig, W. D.; Lee, T. J.; Pitzer, R. M.; Rice, J. E.; Saxe, P.; Scheiner, A. C.; Schaefer, H. F. PSI 2.0.8.; PSITECH, Inc.: Watkinville, GA 30677, 1995. This program is generally available for a handling fee of \$100.
- Siegbahn, P. E. M.; Heiberg, A.; Roos, B. O.; Levy, B. *Phys. Scr.* **1980**, 21, 323.
- Roos, B. O.; Taylor, P. R.; Siegbahn, P. E. M. *Chem. Phys.* **1980**, 48, 157.
- Roos, B. O. *Int. J. Quantum Chem.* **1980**, S14, 175.
- Schaefer, H. F. Ph.D. Thesis, Department of Chemistry, Stanford University, Stanford, CA, April 1969.
- Yamaguchi, Y.; Schaefer, H. F. *J. Chem. Phys.* **1980**, 73, 2310.
- Thomas, J. R.; DeLeeuw, B. J.; Vacek, G.; Crawford, T. D.; Yamaguchi, Y.; Schaefer, H. F. *J. Chem. Phys.* **1993**, 99, 403.
- Besler, B. H.; Scuseria, G. E.; Scheiner, A. C.; Schaefer, H. F. *J. Chem. Phys.* **1988**, 89, 360.
- Bunker, P. R.; Jensen, P.; Yamaguchi, Y.; Schaefer, H. F. *J. Mol. Spectrosc.* **1996**, 179, 263.
- Bunker, P. R.; Jensen, P.; Yamaguchi, Y.; Schaefer, H. F. *J. Phys. Chem.* **1996**, 100, 18088.
- Walsh, A. D. *J. Chem. Soc.* **1953**, 2260.
- Yamaguchi, Y.; Van Huis, T. J.; Sherrill, C. D.; Schaefer, H. F. *Spectrochim. Acta*, in press.
- Badger, R. M. *J. Chem. Phys.* **1934**, 2, 128.
- Badger, R. M. *J. Chem. Phys.* **1935**, 3, 710.